ASSOCIAZIONE NAZIONALE ITALIANA DI INGEGNERIA SISMICA ANIDIS Italian National Association of Earthquake Engineering

XVIII CONVEGNO ANIDIS
L'ingegneria sismica in Italia
ASCOLI PICENO 2019
15-19 Settembre

Preliminary fragility analysis of a r.c. frame school building retrofitted by an external dissipative system

Laura Gioiella[a], Laura Ragni[b], Fabrizio Gara[b], Andrea Dall'Asta[a]
[a] *Scuola di Ateneo di Architettura e Design, Università di Camerino, Viale della Rimembranza, 63100 Ascoli Piceno, Italy*
[b] *Dipartimento di Ingegneria Civile, Edile e Architettura, Via Brecce Bianche, 60131 Ancona, Italy*

Keywords: Italian low-rise schools fragility; external dissipative systems; fluid viscous dampers; pinned-rocking

ABSTRACT
Seismic events occurred in the last decade in Italy led the attention to the evaluation of the health and need of interventions on the existing school buildings heritage, whose collapse or loss in functionality after an earthquake may lead to significant economic and social losses. For this reason, this study focuses on the preliminary fragility assessment of a typical school r.c. frame building, retrofitted through an external configuration based on the use of fluid viscous dampers (FVDs).
The case study is a two elevations moment resisting frame structure, built in Italy in the sixties without seismic code. The external retrofit configuration is a rocking base system consisting of a pinned-rocking braced frames equipped with fluid viscous dampers at their base. Fragility curves, built by accounting for different level of inter-storey drift and for seven intensity measures of the seismic action, provide useful insights about the efficiency and dynamic response of the r.c. frame before and after the retrofitting works.

1 INTRODUCTION

Recent seismic events occurred in Italy (Molise earthquake in 2002, L'Aquila earthquake in 2009 and the Central Italy sequence in 2016) drew the attention to the vulnerability and resilience of public and strategical buildings, especially hospitals and schools. Focusing on the schools, some studies dealing with economic and social losses due to their collapse or loss in functionality after an earthquake have been conducted recently (Dolce 2004 and Rodgers 2012), while some others authors evaluated the performances of the schools after the over mentioned events (Augenti et al. 2002, Dolce et al. 2006, Di Ludovico et al. 2018, Di Ludovico et al. 2019a, Di Ludovico et al. 2019b).

Unfortunately, nowadays, retrofit interventions on Italian school buildings realized without proper seismic detailing or nor in accordance with modern codes provisions, are still limited. Thus, it would be necessary to identify simple procedures to evaluate their vulnerability and the best retrofitting strategies, also by splitting them into proper typological categories, as done for example in Cosentino et al. 2004.

First, schools should be dived into big categories, such as school realized with masonry structure (ancient buildings from 1800 or even earlier, until the end of the second world war) and those with r.c. frame, mainly after the second world war. Then other important aspects should be identified, such as the number of floors or the level of the school (primary rather than, high schools for example) in order to obtain homogeneous typological classes. Successively, for each category, fragility model should be developed in order to perform seismic risk evaluations. These fragility models can be based on simplified or empirical information (Cattari et al. 2014, Lagomarsino et al. 2014), but, for each class, they should be compared with analytical fragility curves obtained by using numerical model of some representative school buildings.

This paper analyses a real three-dimensional case study which is representative of the category of low rise school buildings. The seismic performance of the building is evaluated in its original state in order to develop fragility curves representative of this kind of buildings. Moreover, an external retrofit configuration based on the use of Fluid Viscous Dampers (FVDs), with both linear and non-linear behaviour, is analysed, to show how the use of these devices can reduce the vulnerability of these buildings and increase their resilience, thus, minimising economic and social losses.

2 CASE STUDY AND RETROFIT DESIGN

The case study analysed is a part of the "Parrozzani" school complex of Isola del Gran Sasso, in the central Italy area. Figure 1 reports a planar view of the complex in which the analysed r.c. frame is highlighted in blue. The case study is an r.c. frame building, realized between the '60s and '70s without seismic detailing, and it consists of two elevations above the ground level and one partially underground with reduced dimensions, for an overall height of 11.25 m (each elevation is h_i=3.75 m). The building has already been studied within the ReLUIS project and further information related to the unretrofitted structure assessment can be found in Manfredi and Dolce 2018.

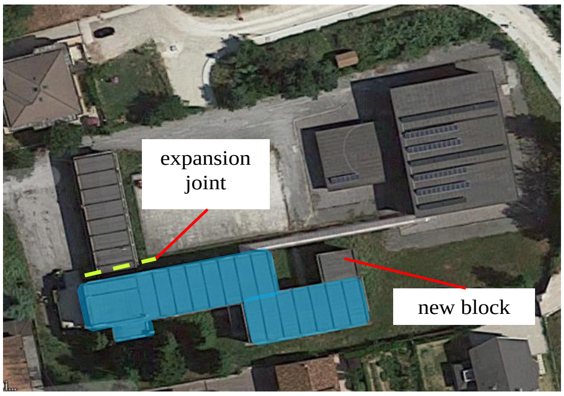

Figure 1. Planar view of the case study

2.1 *Vulnerability assessment of the bare frame*

A 3D FEM model of the bare frame has been built, where beams and columns are modelled with elastic frame element. The non-linear behaviour of the primary elements has been accounted through flexural ductile plastic hinges located at their ends. The modal properties of the frame are reported in Table 1, in terms of period of vibrations and participant masses (M_x, M_y and M_θ), just for the first three vibration modes. The FEM model has been developed with the SAP 2000 programme (computers and Structures 1995). More details about that can be found in Gioiella et al. 2019a.

Table 1. Modal properties of the bare frame.

Mode	T [s]	M_x [-]	M_y [-]	M_Θ [-]
1	0.581	0	0.914	0
2	0.450	0.339	0	0.501
3	0.294	0.536	0	0.374

The vulnerability assessment of the existing building has been conducted through non-linear static analysis, by identifying the the target displacement (d_u), related to the acceptable level of damage, in the capacity curve. For the Y direction, for example, the target displacement is d_u = 0.067 m, corresponding to the activation of a local ductile mechanism involving the staircase. Figure 2 depicts elastic spectrum at the ULS in the acceleration-displacement response spectrum (ADRS) plane, referring to Isola del Gran Sasso, soil category B and topographical category T_1 (T_R=712 years, PGA=0.256g). The reduced demand spectrum, consistently with the damping of the bare frame obtained for the analyzed Y direction (ξ_b=0.11), is also reported.

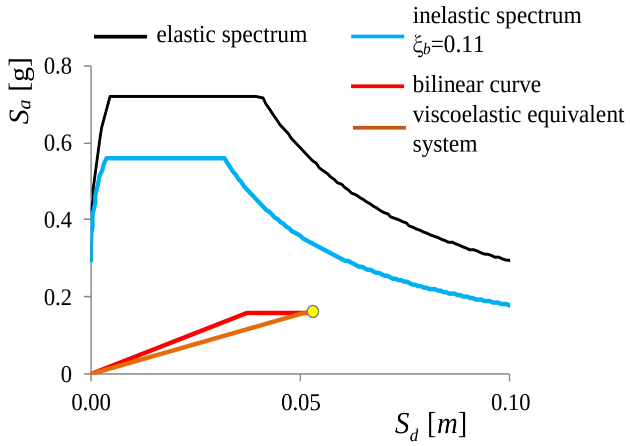

Figure 2. Visco-elastic equivalent system in the ADRS plane for the longitudinal Y direction

The capacity of the viscoelastic system equivalent to the bare frame is lower than the reduced demand spectrum, confirming the need of increasing the seismic performance of the structure. More detail about the vulnerability assessment procedure can be found in Gioiella et al. 2019a.

2.2 *External dissipative system design*

The retrofit of the building is realized by means of an external stiff bracing system pinned at its base and rigidly linked to the existing frame at the floor levels, known as "Dissipative Tower", in order to exploit the rocking motion of the base (RB). The FVDs are located in vertical position at the base of the truss and their deformations are proportional to the vertical displacements of the basement, induced by the rocking motion. The proposed external dissipative bracings contribute only in terms of added damping ξ_d (without modify the overall stiffness of the existing frame), consequently, global dimensions of dampers can be easily determined by finding the additional damping necessary to meet the seismic demand. The design is conducted at the ULS. In the Y direction the required additional damping is $\xi_d = 0.19$, which added to the damping associated with the frame provides a total damping equal to $\xi_{tot} = \xi_b + \xi_d = 0.30$. In the X direction the contribution required for the FVDs is relatively low, equal to $\xi_d = 0.05$, for a corresponding total damping of $\xi_{tot} = 0.17$. However, due to building asymmetry in the X direction, a total damping equal to $\xi_{tot} = 0.13 + 0.12 = 0.25$ is assigned in order to reduce rotational effects in this direction.

Form the additional damping ξ_d, dampers dimension for each considered direction can be determined by using the general expression proposed by ASCE 41-17 (ASCE 2017):

$$\xi_d = \frac{\sum_{j=1}^{N} E_j}{4\pi E_f} \tag{1}$$

where

$$E_f = m_1 \left(d_u \omega_b\right)^2 / 2 \tag{2}$$

describes the maximum strain energy attained by the system associated to the first vibration mode, while the term E_j of the summation, for the case of damper with linear behavior, can be expressed as:

$$E_j = \pi c_{dj} \omega_b s_j^2 \tag{3}$$

and describes the energy dissipated by the j-th device (characterized by the viscous constant c_{dj}) in one complete vibration cycle at frequency ω_b and amplitude s_j, which is the relative displacement between the ends of the device. Since the RB arrangement leads to a linear displacement distribution of the coupled system, due to the stiffening effect of the external truss, the displacement s_j can be expressed as $d_u \cdot z_i / H$, where z_i is the i-th floor height normalized with respect to the total height of the building (H).

In the case of dampers having all the same properties and linear behavior, expression (3) can be rearranged to provide the viscous constant c_d of each damper as follows:

$$c_d = \xi_d \frac{2 m_1 d_u^2 \omega_b}{\sum_j s_j^2} \tag{4}$$

In the case of nonlinear behaviour, the energy dissipated in a cycle by the nonlinear device with constant α can be expressed as:

$$E_j = 2\sqrt{\pi} c_{dj}^{NL} \left(\omega_b\right)^{\alpha} \left(s_j\right)^{1+\alpha} \frac{\Gamma\left(1+\alpha/2\right)}{\Gamma\left(3/2+\alpha/2\right)} \tag{5}$$

where $\Gamma(\cdot)$ is the gamma function. The nonlinear dissipative system has been designed in order to be equivalent to the linear one at the design condition. In particular, the equivalence criterion used requires that the energy dissipated by the two systems is the same for a cycle with angular frequency ω_b and amplitudes s_j. In the case of dampers having all the same properties, the equivalence criterion leads to a viscous constant c_d^{NL} of each nonlinear damper given by the following expression:

$$c_d^{NL} = \frac{\sqrt{\pi}}{2} c_d \left(\omega_b\right)^{1-\alpha} \frac{\sum_j \left(s_j\right)^2}{\sum_j \left(s_j\right)^{1+\alpha}} \frac{\Gamma\left(3/2+\alpha/2\right)}{\Gamma\left(1+\alpha/2\right)} \tag{6}$$

Figure 3 shows the position and the nomenclature (X_i, with i=1÷3 and Y_j, with j=1÷4) of the external structures designed for each direction, namely 3 in transversal X direction (blue lines) and 4 in the Y direction (red lines). The plan dimensions of the bracings are consistent with the dimensions of the spans of the existing frame and they are detailed in Figure 4.

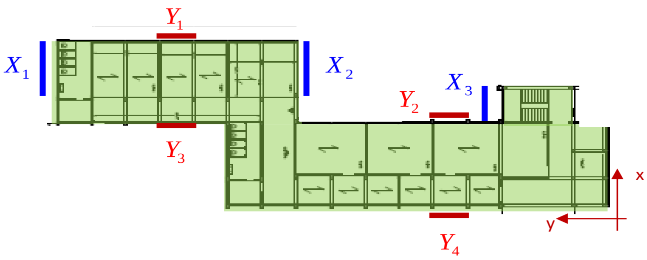

Figure 3. Position of the external dissipative bracings for all the configurations proposed

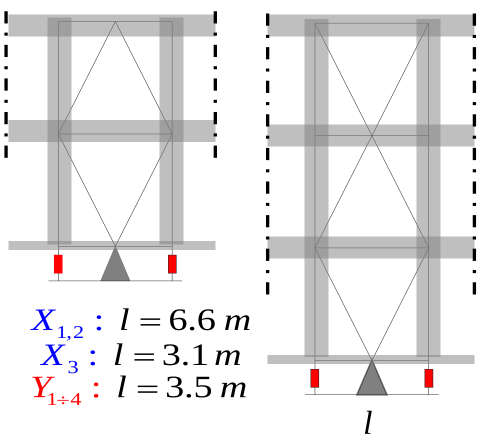

Figure 4. Geometry and number of the FVDs for each type of external structure

The obtained constants for the liner case and the nonlinear one (assuming $\alpha = 0.15$) are reported in Table 2.

Table 2. Viscous constants of dampers

α	X direction		Y direction	
	c_d [kNs/m$^{\alpha}$]	dampers [n°]	c_d [kNs/m$^{\alpha}$]	dampers [n°]
1	1649	6	3278	8
0.15	292	6	334	8

3 INCREMENTAL DYNAMIC ANALYSIS

The seismic performance of the bare frame and of the proposed upgrading configurations is evaluated by means of nonlinear dynamic analyses (time-histories) performed with the SAP2000 program (Computers and Structures 1995). The pivot hysteretic model with a remarkable pinching effect is adopted for the plastic hinges, to describe the degrading mechanism typical of r.c. members with smooth rebars. The FVDs are modelled by two joints links, having a linear behaviour in the case of linear devices and a nonlinear behaviour (exponential Maxwell dampers with α=0.15) for nonlinear devices.

3.1 Seismic input

Regarding the seismic intensity levels, the spectral acceleration (S_a) at the fundamental period of the system is chosen as intensity measure (IM); a set of seven artificial accelerograms (generated by the SIMQKE_GR software, according to the design spectrum at the ULS) is used to simulate the seismic record-to-record variability, and each ground motion sample is scaled to be conditional to seven different IM levels. The first four IM levels identifies seismic events with return periods equal to: 45, 75, 712 and, 1462 years, which also correspond to the limit states of the national design code (i.e., the operational, damage, life safety and collapse limit states, respectively identified as OLS (Operational Limit State), DLS (Damage Limit State), ULS (also called life safe limit state, LSLS) and CLS (Collapse Limit State) for school buildings. The last two IMs, identifying rarer seismic events, are chosen according to the following hazard curve expression:

$$v\left(a_g\right)=k_0\left(a_g\right)^{-k_1} \tag{7}$$

where k_1 and k_0 are set equal to 0.0004 and 2.318 in order to minimize the error in giving the four limit states fixed by the code. Details about the considered IM levels are reported in Table 3.

Table 3. IM levels

	IM1 (OLS)	IM2 (DLS)	IM3 (ULS)	IM4 (CLS)	IM5 (-)	IM6 (-)	IM7 (-)
T_R	45	75	712	1462	2500	5000	10000
ν	0.0222	0.0133	0.0014	0.0007	0.0004	0.0002	0.0001
S_a	0.168	0.218	0.593	0.738	1.000	1.349	1.819

3.2 Analyses results and fragility curves

The most important demand parameter, which is directly related to the damage of both structural and non-structural components, is the inter-storey drift. Thus, it has been monitored before and after the retrofit in order to highlights the increment of the seismic performance of the building. The SEAOC document (SEAOC Vision 2000) has been used as reference document for the thresholds identification. In particular, the following limit states capacity values has been assumed: 0.5% for the DLS, 1% for the ULS and 2% for the CLS.

Figure 5 reports the results of the analyses together with the capacity limits, for the three investigated cases, i.e. the bare frame (BF), the rocking base (RB) system with linear FVDs and the rocking base (RB) system with nonlinear FVDs (RBnl). In particular, the maximum value of inter-storey drift of the structure before and after the retrofit is depicted for each record and for all the IMs, together with the thresholds. The first remark is about the bare frame, which seems to do not have any problem at the OLS and DLS (all the inter-storey drifts are lower than the capacity limit of 0.5% corresponding to non-structural elements damages). At the ULS, instead, it shows inter-storey drifts which significantly overcome the capacity limit of 1%, corresponding to structural damages. After the retrofit, all the inter-storey drifts are lower than the 1% threshold for all the records at the ULS (IM3). Similar results are achieved at the CLS (IM4) for all the records in the linear case and almost all the records in the nonlinear one. For higher values of IM, the differences between the linear and nonlinear cases increase and the results clearly show how the linear devices are more effective in reducing the building inter-storey drifts, which remain below the limit of 2% (corresponding to very severe structural damages) up to IM6. However, it is worth noting that this result is correct and realistic only in case of dampers and external trusses components (included the connections to the bare frame) dimensioned to sustain forces related to this IM. At this regard, it should be noted that in general nonlinear devices are less able to limit displacements but, thanks to their nonlinear behaviour, forces acting on the device are smaller if compared to linear dampers. Obviously, both in the linear and nonlinear case, the stroke capacity limits must be properly designed in order to ensure that the rupture of devices is avoided up to the desired limit state, as shown in the companion paper (Gioiella et al. 2019b).

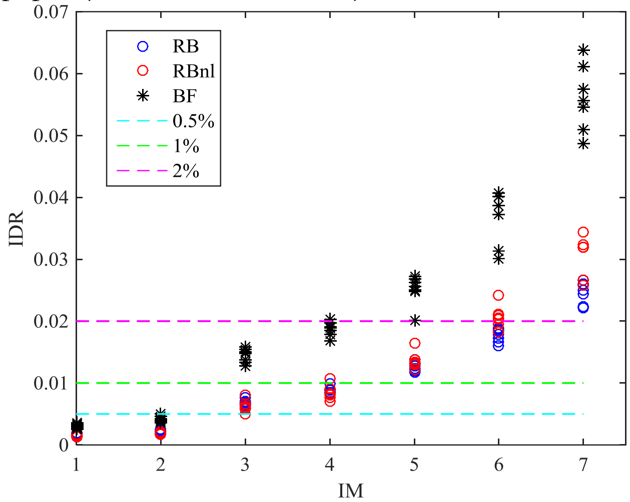

Figure 5. Inter-storey drifts distributions for the different IM and thresholds

The results showed in Figure 5 may be also given in terms of fragility curves (Figures 6 and 7), expressing the probability that the monitored parameter exceeds capacity thresholds as a function of the IM. For the construction of the curves the value of the parameter β, representative of the dispersion, has been assumed equal to 0.4 in accordance with the standard ASCE 7-16.

It can be observed how the fragility curves relevant to the severe (Figure 6) and very severe structural damages (Figure 7) are strongly affected by the retrofitting. In particular, it is confirmed that the dissipative RB system with linear devices is more efficient in reducing the building vulnerability.

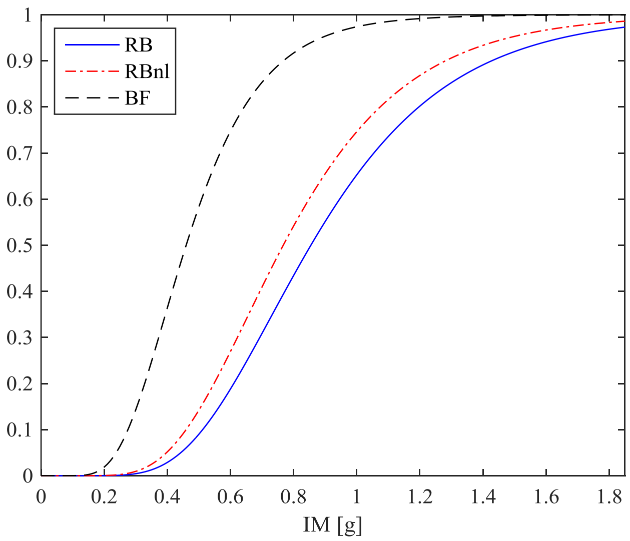

Figure 6. Fragility curve for the inter-storey drift capacity threshold of 1%

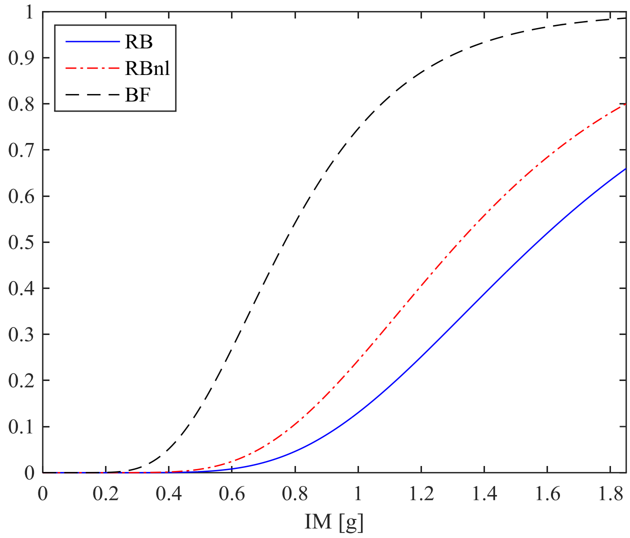

Figure 7. Fragility curve for the inter-storey drift capacity threshold of 2%

4 CONCLUSIONS

In this paper a first estimation of fragility curves related to an r.c. frame building representative of low rise Italian schools, before and after the retrofitting works, has been done. Results have shown that fragility curves relevant to the severe and very severe structural damages are strongly affected by the retrofitting and that the dissipative RB system with linear devices is more efficient in reducing the building vulnerability. However, results should be integrated with fragility curves of the devices, both in terms of forces and displacements. To do this, capacity limits in terms of forces and strokes should be defined, according to current design code prescriptions.

REFERENCES

Augenti, N., Cosenza, E., Dolce, M., Manfredi, G., Masi, A., Samela, L., 2004. Performance of School Buildings during the 2002 Molise, Italy, Earthquake. *Earthquake Spectra*, **20**(S1), S257-S270.

Computers and Structures, Inc., 1995. SAP2000, Structural Analysis Program, University Ave., Berkeley, CA.

Di Ludovico, M., Digrisolo, A., Moroni, C., Graziotti, F., Manfredi, V., Prota, A., Dolce, M., Manfredi, G., 2018. Remarks on damage and response of school buildings after the Central Italy earthquake sequence. *Bulletin of Earthquake Engineering*.

Di Ludovico, M., Santoro, A., De Martino, G., Moroni, C., Prota, A., Dolce, M., Manfredi, G., 2019a. Cumulative damage to school buildings following the 2016 central Italy earthquake sequence. *Bollettino di Geofisica Teorica ed Applicata*, **60**(2), 165-182.

Di Ludovico, M., De Martino, G., Santoro, A., Prota, A., Manfredi, G., Calderini, C., Carocci, C., da Porto, F., Dall'Asta, A., De Santis, S., Fiorentino, G., Digrisolo, A., Dolce, M., Moroni, C., Ferracuti, B., Ferretti, D., Graziotti, F., Penna, A., Mannella, A., Marini, A., Mazzotti, C., Sorrentino, L., 2019b. Usability and damage assessment of public buildings and churches after the 2016 Central Italy earthquake: The ReLUIS experience. *7th International Conference Earthquake Geotechnical Engineering for Protection and Development of Environment and Constructions*, June 17-20, Rome, Italy.

Dolce, M., 2004. Seismic safety of schools in Italy. *OECD Ad Hoc Expert's Group Meeting on Earthquake Safety in Schools*, Paris, France.

Dolce, M., Kappos, A., Masi, A., Penelis, G., Vona, M., 2006. Vulnerability assessment and earthquake damage scenarios of the building stock of Potenza (Southern Italy) using Italian and Greek methodologies. *Engineering Structures*, **28**, 357-371.

Cosentino, N., Manieri, G., Benedetti, A., 2004. A brief review of school typologies in Italy: specific vulnerability and possible strategies for seismic retrofitting. *OECD Ad Hoc Expert's Group Meeting on Earthquake Safety in Schools*, Paris, France.

Cattari, S., Lagomarsino, S., Ottonelli, D., 2014. Fragility curves for masonry buildings from empirical and analytical models. *2nd European Conference on Earthquake Engineering and Seismology*, August 25-29, Istanbul, Turkey.

Lagomarsino, S., Cattari, S., 2014. Fragility functions of masonry buildings. In Pitilakis K, Crowley H, Kaynia A (eds) SYNER-G: typology definition and fragility functions for physical elements at seismic risk, buildings, lifelines, transportation networks and critical facilities series, *Geothechnical, Geological and Earthquake Engineering*, **27**, 111–156.

ASCE Standard ASCE/SEI 41-17: Seismic evaluation and retrofit of existing buildings. American Society of Civil Engineers, 2017.

SEAOC. Vision 2000: performance based seismic engineering of buildings. San Francisco: Structural Engineers Association of California; 1995.

Rodgers, J:E:, 2012. Why Schools are Vulnerable to Earthquakes. *15th World Conference on Earthquake Engineering*, September 24-28, Lisbon, Portugal.

Manfredi, G., Dolce, M., 2018 The state of Earthquake Engineering Research in Italy: the ReLUIS-DPC 2014-2018 Project.

Gioiella, L., Tubaldi, E., Ragni, L., Gara, F., Dall'Asta, A., 2019a. The seismic retrofit by external dissipative: a case study. *COMPDYN 7th ECCOMAS Thematic Conference on Computational Methods in Structural Dynamics and Earthquake Engineering*, June 24-26, Crete, Greece.

Gioiella, L., Ragni, L., Dall'Asta, A., Scozzese, F., 2019b. Reliability of a r.c. frame equipped with linear and nonlinear fluid viscous dampers. *XVIII Convegno ANIDIS L'ingegneria sismica in Italia*, September 15-19, Ascoli Piceno, Italy.

ASCE Standard ASCE/SEI 7-16: Minimum Design Loads and Associated Criteria for Buildings and Other Structures. American Society of Civil Engineers, 2017.